Mathematical modelling of a kenaf harvester

Thomas Adedayo Ayorinde[1, 2*], Oseni Kehinde Owolarafe[2]

(1. Bioresources Development Center, P.M.B 3524, Ogbomoso, National Biotechnology Development Agency, Abuja, Nigeria; 2. Department of Agricultural and Environmental Engineering, Obafemi Awolowo University, Ile-Ife, Nigeria)

Abstract: The aim of this research article is to develop a mathematical model of the impact cutting behaviour of a circular cutting blade on kenaf stems. The model predicts and validates the effects of crop maturity and varieties on the cutting torque, power, and energy required during kenaf harvesting. The developed mathematical model for predicting the cutting torque, power, and energy for an improved tractor mounted kenaf harvester was found to be accurate. The cutting torque, power, and energy consumed during kenaf harvesting increase steadily with increased maturity for all varieties of kenaf. Also, the highest cutting torque, power, and energy during the harvesting of Ifeken 400 ranged from 1.51 Nm to 3.36 Nm, 10.19 kW to 22.61 kW, and 1.77 Joules to 3.94 Joules.

Keywords: kenaf, harvester, tractor, forward speed, field efficiency

Citation: Ayorinde, T. A., and O. K. Owolarafe. 2024. Mathematical modelling of a kenaf harvester. Agricultural Engineering International: CIGR Journal, 26 (2):113-124.

1 Introduction

Global economic growth has driven an increase in energy demand, predominantly relying on fossil fuels and polymers, thereby causing bioresource depletion and environmental degradation. These environmental concerns have spurred extensive research into sustainable, efficient, eco-friendly, and renewable composites. Which has become a very active and highly promising field in materials science (Ayorinde and Olasebikan, 2020; Yaghoobi and Fereidoon, 2018).

Kenaf (*Hibiscus cannabinus L.),* an annual crop that originates from Africa, expanded to Asia during the 1900s, and later to the USA in the 1940s. Belonging to the Malvaceae family, it shares botanical ties with cotton, okra, sorghum, and roselle. It has been globally identified as a valuable industrial crop, providing a natural fibre source. Its capacity for carbon dioxide absorption and water purification, enhances its application as an eco-friendly alternative (Ayadi et al., 2017; Ayorinde and Owolarafe, 2023). It finds extensive applications across various industries including, automotive, agriculture, construction, chemicals, and packaging industries. It can be blended with synthetic fibre for carpet production and utilised in diverse forms, such as oil absorbents, animal bedding, and horticultural mixes. Its versatility also extends to providing raw materials for products like jute bags, paper, twine, and plaster of Paris. Kenaf is highly esteemed in its cultivation areas for its versatility and diverse applications, contributing significantly to job creation and the promotion of sustainable practices in Africa (Ayadi et al., 2017; Ayorinde and Owolarafe, 2023b; Ghahraei et al., 2011; Müssig et al., 2024).

The process of plant material cutting, especially stalk plants like kenaf, has been identified as one of the most important areas in crop and forage harvesting. The most widely used plant-cutting

Received date: 2023-09-15 **Accepted date:** 2024-03-22

* **Corresponding author: Thomas Adedayo Ayorinde,** Ph.D., National Biotechnology Development Agency, Abuja, Nigeria. Email: ayorindeadedayo@gmail.com. Tel: +2348132646687.

devices are harvesters, chaff cutters, and mowers (Zastempowski and Bochat, 2014). So, research into the design and improvement of harvest and postharvest technologies for plant stalk harvesting remains a significant area to explore. In improving the efficiency of this machines, extensive research into the mechanics of the plant material is required, which neglects the fact that crop stalks are biological materials with complex structures, anisotropy, viscoelasticity, and rheology (Ayorinde et al., 2019; Dongdong, 2016; Ghahraei et al., 2011).

The process for kenaf stalk harvesting involves cutting the plant stem using a knife, which shears the material between a moving blade and a countershear. To enhance the design of the kenaf harvester, it is crucial to minimise cutting force and energy while preserving the quality of the harvested plant stem. This entails examining the relationship between the cutting device's mechanical parameters and the crop's characteristics, including physical size, tensile strength, compressive strength, and shear strength. The accurate estimation of these factors will establish a framework for developing a mathematical equation that incorporates the crop stalk's morphology into a mechanical structure, that enable the prediction of cutting force, power, and energy required during stem harvesting (Dongdong, 2016; O'dogherty, 1982; Srivastava et al., 2006; Uche et al., 2018).

From literature, optimization of cutting force and energy was considered under different cutting tool mechanisms, and cutting speed was evaluated in relations to the cutting blade and the stem geometry. But the study was not suitable for large shrubs like kenaf which have to consider counterbar configuration, stem deflection, resistance of the crop stem, and other dynamic factors like; the instantaneous cutting force, torque, and motion over time (Guarnieri et al., 2007).

An improved tractor mounted kenaf harvester which was design using a circular cutting blades, consist of spur and bevel gears, chains and sprockets, and shafts as shown in the power train in Figure 1. The aim of this research is to develop a mathematical model of the impact cutting behavior of the circular cutting blade on kenaf stem. It will also predict and validate the effect of the crop maturity and varieties on the cutting torque, power and energy required during kenaf harvesting using the kenaf harvester developed by Ayorinde and Owolarafe (2023a).

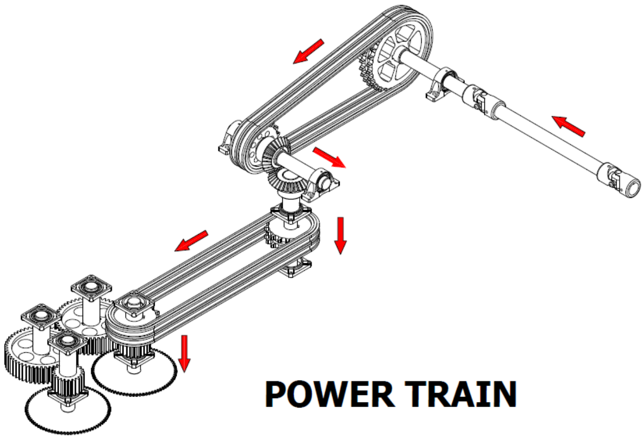

Figure 1 Power train of the kenaf harvester

2 Model development

2.1 Kenaf plant structure

The structure of a plant's stem is crucial in understanding how it responds to cutting force. Although plant materials have not been extensively studied in terms of engineering properties compared to metals like steel, there have been some investigations into kenaf material. Kenaf plants feature a single, straight, and branchless stalk comprising an inner woody core surrounded by an outer fibrous bark. Typically, the stalk as shown in Figure 2, contains approximately 30% bast fiber and 70% core fiber, with the bast fiber concentrated in the bark and the core fiber located at the stem's center (Ishaket et al., 2010; Srivastava et al., 2006).

In studies, kenaf fiber bundles with diameters ranging from 50 to 150 µm and lengths of 500 mm have been utilized. Examination of the cutting characteristics of kenaf stems at various moisture content levels (35%, 55%, and 72%) has revealed notable differences. For instance, at 35% moisture content, the maximum cutting force and shearing energy were measured at 1584.55 N and 8.75 J, respectively, whereas at 72% moisture content, these values decreased to 694.86 N and 3.50 J. The Young's modulus, which indicates stiffness, ranged between 67.59 and 234.24 MPa. Turgor pressure within plant cells, influenced by moisture content, significantly impacts the plant's rigidity and strength, which constituents plant stiffness factor(Persson, 1987). Generally, plants exhibit greater size and strength nearer to the ground, providing resistance against wind loading and stability during harvesting(Ayorinde et al., 2019; Ayorinde and Owolarafe, 2023; Dauda et al., 2015; Raji and Aremu, 2017).

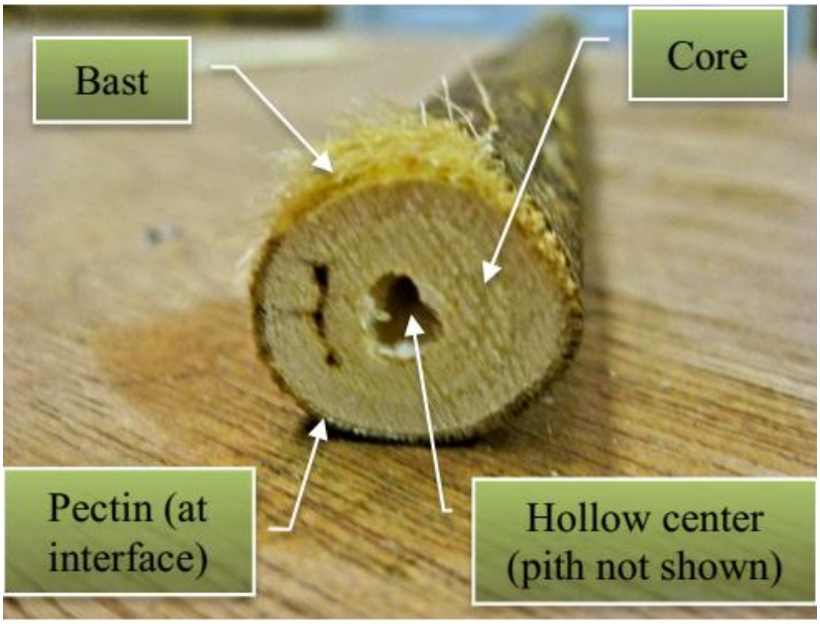

Figure 2 Cross-section of kenaf stalk (Sheldon, 2014)

2.2 Mechanics of the kenaf stem cutting

The effectiveness of the stem cutting depends on the knife or blade characteristics, the cutting force applied, some physical, and mechanical properties of the stem (Gupta and Oduori, 1992; O'dogherty, 1982). Initial penetration of the cutting blade on the plant stem starts the harvesting process as shown in Figures 3 and 4. With further knife penetration, considerable stem buckling and compression occurs depending on the blade sharpness and speed (Chattopadhyay and Pandey, 2001; McRandal and McNulty, 1978).

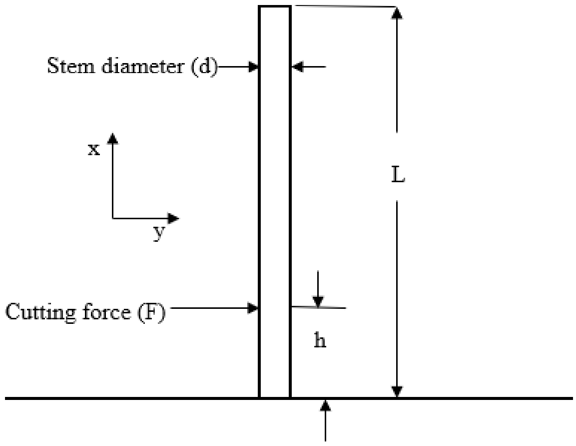

Figure 3 Model of kenaf stem subjected to a cutting force (F)

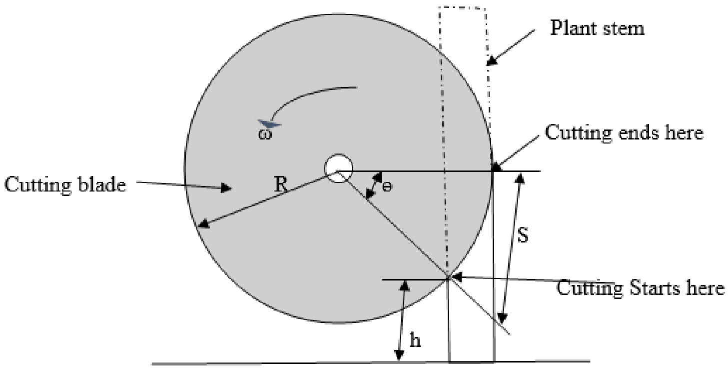

Figure 4 Model of the kenaf stem subjected to a cutting force by a rotary blade cutter

2.3 Assumptions for the model development

The mathematical model for the kenaf harvester was developed based on the following assumptions:

1) The mass of the severed plant stalk was concentrated at the point where the cutting force was applied;

2) The counter shear is provided entirely by the plant stem fixed to the ground and stems along the crop row;

3) The blade tip makes the impact and n represent the number of blades needed to sever the plant stem.

Some of the parameters identified for modelling include.

1) Cutting height, *h*;

2) Cutting circle radius, *R*;

3) Cutting arc, *S*;

4) Cutting angle, *θ*;

5) Rotational speed, *ω*;

6) Cutting force required for unit penetration, *K*;

7) Time required to cut the stalk, *t*;

8) Peripheral cutting speed of blade, V_0.

2.4 Development of the equation

The cutting force applied to the kenaf stem, as shown in Figure 3, was applied to overcome blade inertia and friction, due to the shear property of the plant stalk (Soleimani et al., 2023). Based on Newton's second law of motion, the cutting force during impact is given by Equation (1) (Chattopadhyay and Pandey, 2001).

$$F_T = £\, m\frac{d^2x}{dt^2} \tag{1}$$

Where: F_T is the cutting force in newton, £ is the factor depending on the characteristics of the plant stalk being cut, *m* is the mass of the cut plant separated from the stubble in Kilogram, *x* is the deflection in meters of the cut plant stalk along the X-axis in time t; and d^2x/dt^2 is the acceleration of the cut plant along the X-axis.

Based on the third assumption, the total cutting force applied to cutting kenaf stem with crop stem diameter (*d*) at cutting height (*h*) is given by Equation (2):

$$F_T = n£\, m\frac{d^2x}{dt^2} \tag{2}$$

During impact cutting, the cutting force, F_T, must be supported by a countershear, which is provided entirely by the plant, through its stump below and the inertia above the cutting point (Srivastava et al., 2006). A stiffness factor f_s is the plant support, which is determined by the mechanical property of the stem (Chattopadhyay and Pandey, 2001). The plant stem deflected by the cutting blade impact during cutting acquires and maintain a peripheral speed (speed at a point on the circumference of the saw blade), which is equal to the energy required for the cutting of the stem and energy expended to overcome friction (Yiljep and Mohammed, 2005) is given by Equation (3) (Totten and Millier, 1966):

$$F_T = f_s\int F dt = f_s\int ma\, dt = f_s mv = f_s m(v_f - v_i) = f_s m v_0 \tag{3}$$

where: V_0 is the peripheral cutting speed of the blade, V_f is the final velocity of the blade section after impact, V_i is the velocity of the blade before impact, and f_s is the stiffness factor that resists the stem deflection during impact and depends on the elastic properties of the plant material.

During impact cutting, Equation 2 must be equal to Equation 3.

$$n\varepsilon m\frac{d^2x}{dt^2} - f_s m v_0 = 0$$

$$n\varepsilon\frac{d^2x}{dt^2} - f_s v_0 = 0$$

$$n\varepsilon\frac{dx}{dt} - f_s v_0 t = 0 \tag{4}$$

Where: C_1 is the integration constant. At t = 0, dx/dt = Vi = 0. Hence, the value of the integration constant is zero, and Equation 4 becomes

$$\frac{dx}{dt} = \frac{f_s v_0 t}{n\varepsilon} \tag{5}$$

Integrating Equation (5), we have:

$$n\varepsilon\int dx - f_s v_0\int t\, dt = c_2$$

$$n\varepsilon x - f_s v_0\frac{t^2}{2} = c_2 \tag{6}$$

where: C_2 is the integration constant.

Again, at *t* = 0, the deflection *x* is zero, and therefore the value of the second integration constant is also zero. Hence, Equation 6 is written as

$$X = \frac{f_s v_0 t^2}{2n\varepsilon} \tag{7}$$

From Figure 3, the cutting blade cut the stem along the circumference S for the complete cutting of the plant stalk. The length of the cutting arc S is given by:

$$S = R\theta = R\cos^{-1}(\frac{R-d}{R}) \tag{8}$$

From Figure 4,

$$x = v_0 t - S = v_0 t - R\theta \tag{9}$$

Equating Equations 7 and 9

$$\frac{f_s v_0 t^2}{2n\varepsilon} = v_0 t - R\theta$$

$$t^2 - \frac{2n\varepsilon t}{f_s} + \frac{2n\varepsilon R\theta}{f_s v_0} = v_0 t - R\theta \tag{10}$$

Solving quadratic equation 10 using the formula method

$$t = \frac{-b \pm \sqrt{b^2 - 4ac}}{2a}$$

$$t = \frac{\frac{2n\varepsilon}{f_s} \pm \sqrt{\frac{4n^2\varepsilon^2}{f_s} - \frac{8n\varepsilon R\theta}{f_s v_0}}}{2}$$

$$t = \frac{\frac{2\varepsilon}{f_s} \pm \sqrt{\frac{4n^2\varepsilon^2}{f_s^2}(1 - \frac{2Rf_s\theta}{V_0 n\varepsilon})}}{2}$$

$$t = \frac{\frac{2n\varepsilon}{f_s} \pm \frac{2n\varepsilon}{f_s}\sqrt{(1 - \frac{2Rf_s\theta}{V_0 n\varepsilon})}}{2}$$

$$t = \frac{\frac{2n\varepsilon}{f_s}\left(1 \pm \sqrt{(1 - \frac{2Rf_s\theta}{V_0 n\varepsilon})}\right)}{2}$$

$$t = \frac{n\varepsilon}{f_s}\left(1 \pm \sqrt{(1 - \frac{2Rf_s\theta}{V_0 n\varepsilon})}\right)$$

A possible solution is:

$$1 - \frac{2Rf_s\theta}{v_0 n\varepsilon} = 0$$

Therefore,

$$\varepsilon = \frac{2Rf_s}{v_0 n} = \frac{2Rf_s}{v_0}\cos^{-1}\frac{R-d}{R} \tag{11}$$

The model in Figure 5 illustrates the typical shape of the cutting force displacement with different stalk stiffness along the plant stem diameter (*d*). This model accounts for the force acting on the cutting blade and the energy expended at different stages of the cutting process (Guarnieri et al., 2007; Zastempowski and Bochat, 2014).

From Figure 5, $K = \frac{F_T}{S/2} = \frac{2F_T}{R\theta}$

Where: K is the cutting force per unit depth of knife penetration into the stem, as shown in Figure 5.

From the geometry in Figure 5, the totaling blade cutting displacement ($R\theta$) on Figure 4 is equal to ($V_0 t$-x) on the cutting force displacement model.

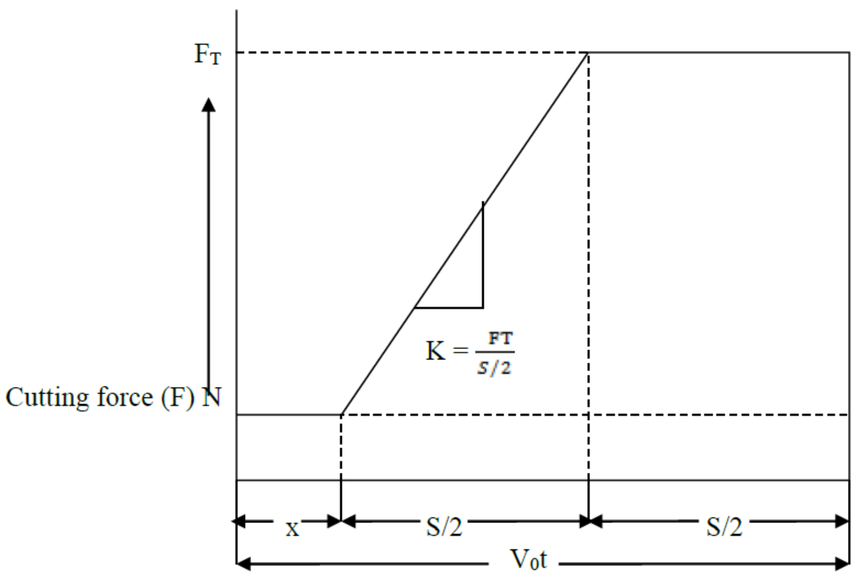

Figure 5 Model of the cutting force distribution by the cutting blade

$$F_T = \frac{KR\theta}{2} \tag{12}$$

$$F_T = \frac{KR\theta}{2} \tag{13}$$

Now, from Equation 2,

$$F_T = n\varepsilon m\frac{d^2x}{dt^2} = n\varepsilon(L-h)\rho\frac{d^2x}{dt^2} \tag{14}$$

Note that $m = \rho L = \rho(L-h)$

Where: L is the total height of the plant stalk from the ground level, h is the cutting or stubble height, and ρ is the linear density of the plant stalk.

Equating Equations 13 and 14,

$$\frac{k(v_0 t - x)}{2} = n\varepsilon(L-h)\rho\frac{d^2x}{dt^2}$$

$$\frac{d^2x}{dt^2} + \frac{K}{2(L-h)n\rho\varepsilon}(V_0 t - x) = 0$$

$$\frac{d^2x}{dt^2} + ax - V_0 at = 0 \quad (15)$$

Where: $a = \frac{K}{2(L-h)n\rho\varepsilon}$

Equation 15 being a non-homogenous second-order differential equation, the solution is:

$$x = V_0(t - 1/\sqrt{a})\sin t\sqrt{a}$$

Cutting is completed when the knife edge travels a distance S, as shown in Figure 2, such that

$$V_0 t - x = S = R\theta = R\cos^{-1}(\frac{R-d}{R})$$

So,

$$V_0 t - V_0(t - 1/\sqrt{a})\sin t\sqrt{a} = R\cos^{-1}(\frac{R-d}{R})$$

$$(V_0/\sqrt{a})\sin t\sqrt{a} = R\cos^{-1}(\frac{R-d}{R})$$

Therefore,

$$V_0 = \frac{R\cos^{-1}(\frac{R-d}{K})}{(1/\sqrt{a})\sin t\sqrt{a}} \quad (16)$$

Now, from Equation 16, it can be seen that the cutting speed V_0 is a minimum V_{min} (critical cutting speed) when $\sin t\sqrt{a} = 1$.

Therefore, Equation 16 becomes

$$V_{\min} = \sqrt{\frac{K}{2(L-h)n\rho\varepsilon}}(R\cos^{-1}\frac{R-d}{R})$$

$$K = \frac{2(L-h)n\rho\varepsilon v_{\min}^2}{R^2(\cos^{-1}(R-d)/R)^2} \quad (17)$$

Combining Equations 8, 10, 12, and 17 gives

$$F_T = \frac{2(L-h)n\rho f_s v_{\min}^2}{v_0} \quad (18)$$

The time t_c required for cutting the stem can be determined from Equation 16 as follows:

$$V_0 = \frac{R\cos^{-1}\frac{R-d}{R}}{(1/\sqrt{a})\sin t_c\sqrt{a}}$$

Or $t_c = \frac{1}{\sqrt{a}}\sin^{-1}\left[\frac{R\sqrt{a}}{V_0}\cos^{-1}\frac{R-d}{R}\right]$

$$T_c = \frac{R\cos^{-1}(R-d)/R}{V_{\min}}\sin^{-1}\frac{V_{\min}}{V_0} \quad (19)$$

The cutting torque T_r at the rotor shaft due to the cutting force F_T from the model is given by

$$T_r = F_T R = \frac{2(L-h)n\rho f_s V_{\min}^2 R}{V_0} \quad (20)$$

Similarly, the cutting power P_c is given by

$$P_c = F_T V_0 = 2(L-h)n\rho f_s V_{\min}^2 R \quad (21)$$

The cutting energy E_c required to sever the stem is given by

$$E_c = P_c t_c = 2 f_s R V_{\min}(L-h)n\rho\cos^{-1}\frac{R-d}{R}\sin^{-1}\frac{V_{\min}}{V_0} \quad (22)$$

3 Materials and methods

3.1 Experimental procedure

This experiment was conducted at the Teaching and Research Farm of the Obafemi Awolowo University, Ile-Ife, Nigeria. The improved harvester was mounted on a tractor, with the torque transducer installed on the PTO shaft of the kenaf harvester. The cutting blade speed was set at the critical cutting speed of 0.75 m s^{-1} as per the existing literature. The measurements of experimental cutting torque, power, and energy were taken at weeks 10, 12, 14, and 16 across three kenaf varieties: Cuba 108, Ifeken DI 400, and Ifeken 400. At the time of harvest, the average stem moisture content, height, and diameter were recorded as 69%, 2.7 m, and 20.55 mm, respectively. Predicted and experimental values of cutting torque, power, and energy were plotted on a graph, and the validity of the equation was assessed by examining the coefficient of determination (R^2).

3.2 Determination of the predicted value of cutting torque, power, and energy

The field variables used for estimating the plant stalk stiffness factor in equations 11, 17, and 18, and the predicted values of cutting torque, power, and energy in equations 20, 21, and 22 are shown in Table 1.

3.3 Determination of the experimental values cutting torque, power, and energy

The cutting torque required to cut the plant stalk by impact was sensed by the torque transducer mounted on the PTO shaft. The predicted value of cutting torque was calculated using Equation (23).

$$T_r = F_T R \quad (23)$$

The power required was then determined from the recorded torque and rotational speed of the PTO shaft on the tractor. It was plotted against the predicted value of cutting power obtained from Equation (24). While, the time required to cut the kenaf stalk was estimated from Equation (25).

$$P_c = F_T V_0 \quad (24)$$

$$t = \frac{s}{v_0} \quad (25)$$

Where: t is the time required to cut the stalk completely at the cutting height, S is the length of the cutting arc, and V_0 is the cutting speed of the blade.

The energy required to sever the plant stalk in equation 26 was determined by estimating the product of the determined power of Equation (24) and the cutting time of Equation (25). The deflection of the stem was neglected. Zhao et al. (2022) showed that cutting speed and time perfectly influence energy consumption during cutting.

$$E_c = P_c t_c \quad (26)$$

Table 1 Prevailing crop and field conditions during field evaluation of kenaf harvester

Parameter	Kenaf varieties		
	Cuba 108	Ife ken Di 400	Ife ken 100
Age of plants (weeks)	10-16	10-16	10-16
Row spacing (m)	0.3 × 0.1	0.3 × 0.1	0.3 × 0.1
Average numbers of stem in 1 row	190 – 240	100 – 170	100 – 120
Plant population on the field (plants ha^{-1})	333,333	333,333	333,333
Approximate yield of kenaf stem (t ha^{-1})	18.518	21.43	16.67
Average height of kenaf stem above ground surface (m)	2.7	2.9	2.5
Average cutting height of kenaf stem above ground surface (cm)	15	15	15
Average moisture content of kenaf stem at harvest time (%) wb	69	72	62
Average diameter of kenaf stems (mm)	20.55	21.06	18.98

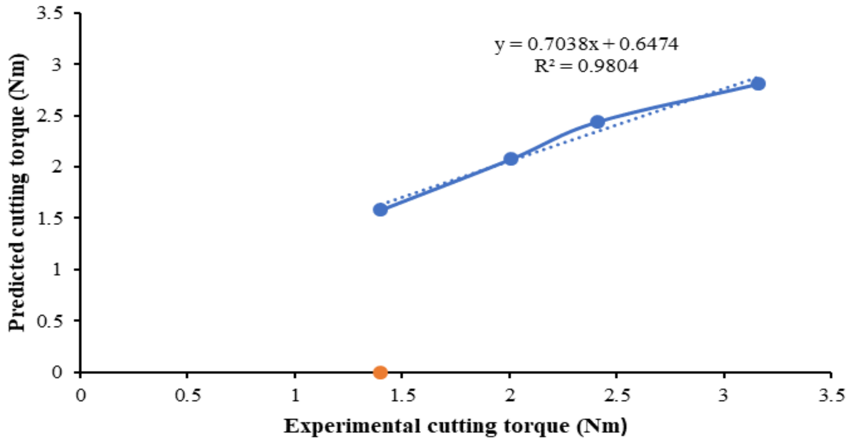

(a) Cuba 108

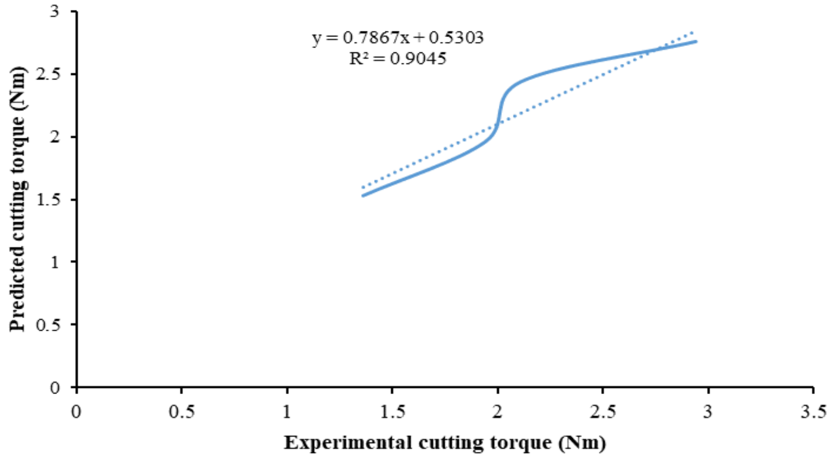

(b) Ifeken DI 400

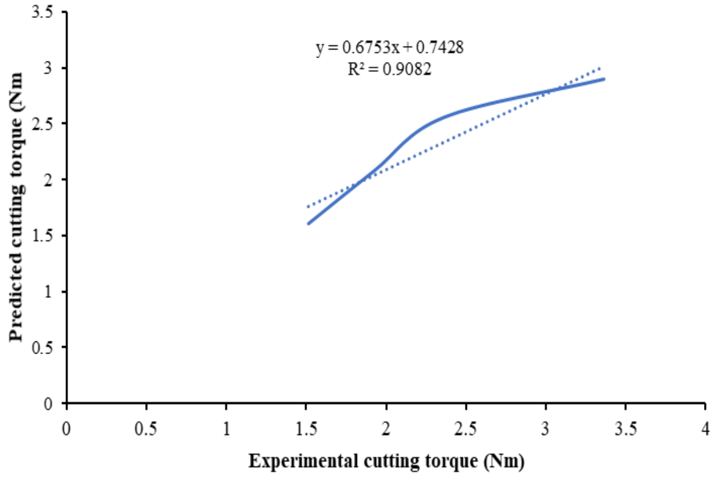

(c) Ifeken 400

Figure 6 Cutting torque model validation

4 Results and discussion

4.1 Model validation of the cutting torque equation

Figure 6 illustrates the validation of the cutting torque mathematical model across the three varieties of kenaf studied. The model shows a consistent increase in cutting torque from 1.40 Nm to 3.16 Nm, 1.36 Nm to 2.94 Nm, and 1.51 Nm to 3.36 Nm for Cuba 108, Ifeken DI 400, and Ifeken 400, respectively, as the crop matures from week 10 to 16. This increasing trend is observed uniformly across the three varieties and aligns with the findings from previous studies by Dauda et al. (2015) and Sahni and Jena (2022). This trend underscores the influence of turgor pressure within the plant, which increases as the crop matures and significantly impacts plant rigidity and strength, thus contributing to the plant stiffness factor. Consequently, greater cutting torque is required as the plant matures (Chattopadhyay and Pandey, 2001; Raji and Aremu, 2017; Srivastava et al., 2006).

The coefficient of determination (R^2) of the models shows their validity. R^2 values for Cuba 108, Ifeken DI 400, and Ifeken 400 are 0.9804, 0.9045, and 0.9082, respectively, greater than the 0.7 coefficient threshold. This suggests that the mathematical model can reliably predict the cutting torque required during kenaf harvesting.

4.2 Model validation of the cutting power equation

The model validation of the cutting power equation is shown in Figure 7 for the three varieties of kenaf under study. It is observed that the cutting power increases steadily from 9.40 kW to 21.24 kW, 9.17 to 19.77 kW, and 10.19 kW to 22.61 kW for Cuba 108, Ifeken DI 400, and Ifeken 400, respectively, as the crop matures from weeks 10 to 16. The steady increase in power required to cut kenaf stem during harvesting is attributed to stem stiffness with crop maturity, which aligns with the observations of Ghahraei et al. (2011), Gupta and Oduori (1992), and Veikle (2011). The coefficient of determination of the model shows that the equation is valid because the R^2 for the three varieties under study is higher than 0.7, as shown in Figure 7.

4.3 Model validation of the cutting energy equation

The cutting energy model validation illustrated in Figure 8 shows the relationship between the predicted and experimental cutting energy required during kenaf harvesting (Kushwaha et al., 1983; Yilmaz et al., 2009a). The kenaf stalk cutting energy consumption for Cuba 108 increased from 1.64 Joules to 3.70 Joules, for Ifeken DI 400 increased from 1.59 Joules to 3.44 Joules, and for Ifeken 400 increased from 1.77 Joules to 3.94 Joules, as the crop matures from week 10 to 16. The steady increase in energy consumption responds to cutting resistance due to the variation in stalk cross-sectional area and texture, primarily in the fibrous and lignin content of the stem, as reported by Yilmaz et al. (2009) and Soleimani et al. (2023). All the model coefficients of determination (R^2) for Cuba 108, Ifeken DI 400, and Ifeken 400 are 0.9808, 0.9115, and 0.9073, respectively, which are closer to 1 than 0.7. This shows that the equation modelled for predicting the values of energy consumption during kenaf harvesting is valid and can accurately predict cutting energy during harvesting.

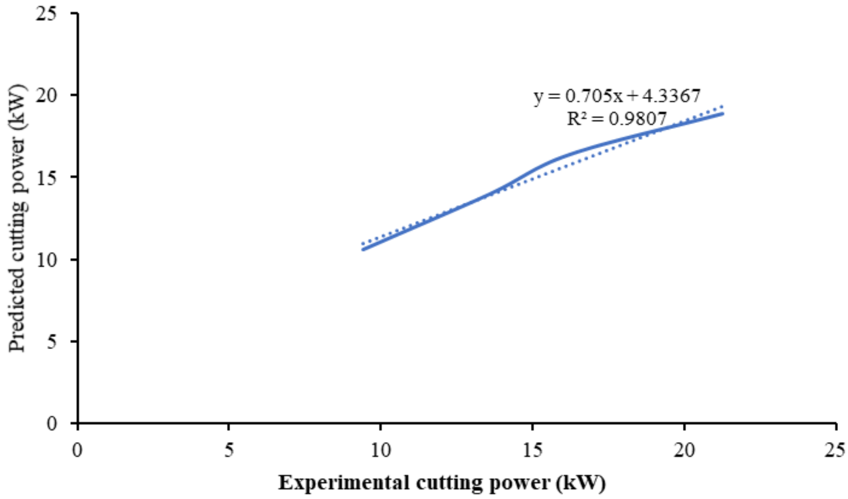

(a) Cuba 108

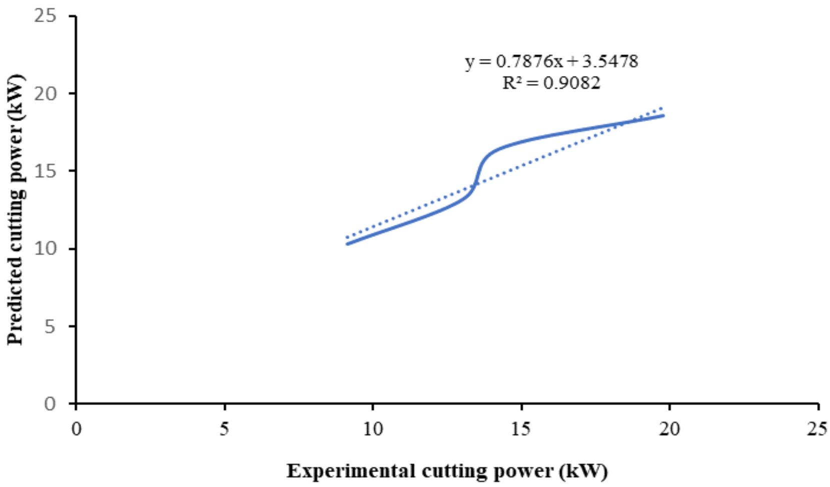

(b) Ifeken DI 400

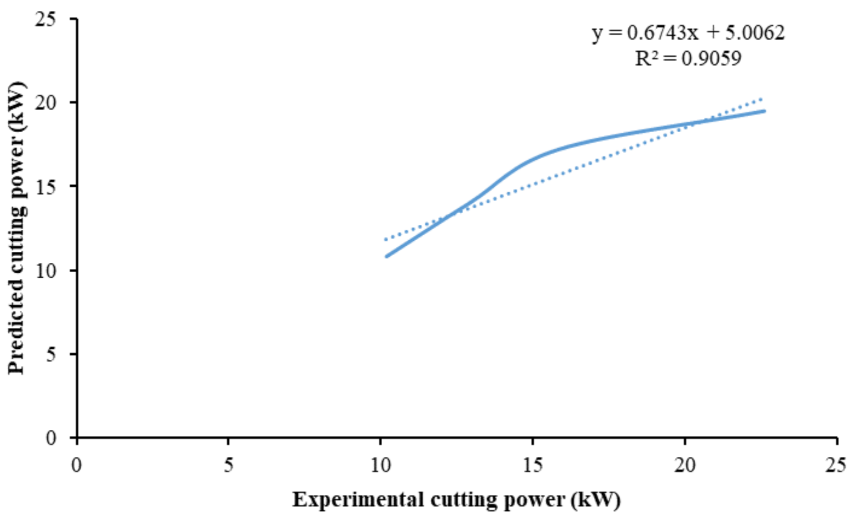

(c) Ifeken 400

Figure 7 Cutting power model verification

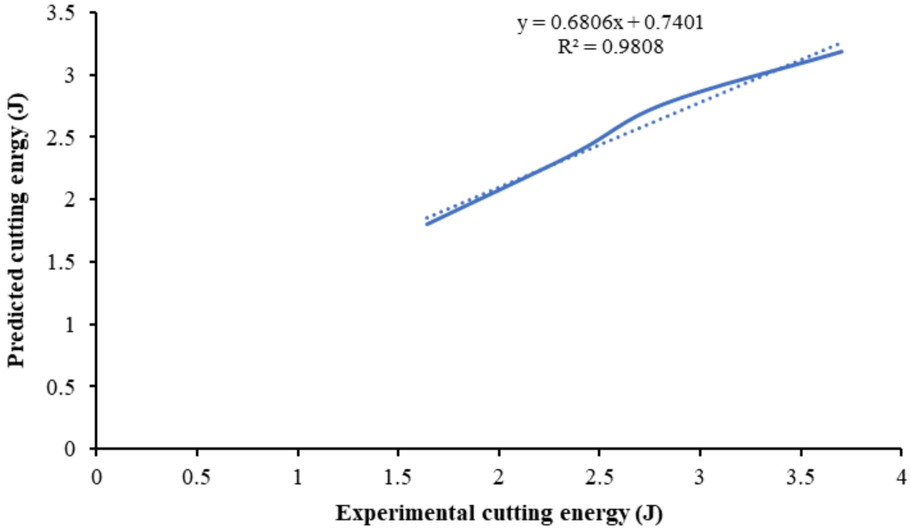

(a) Cuba 108

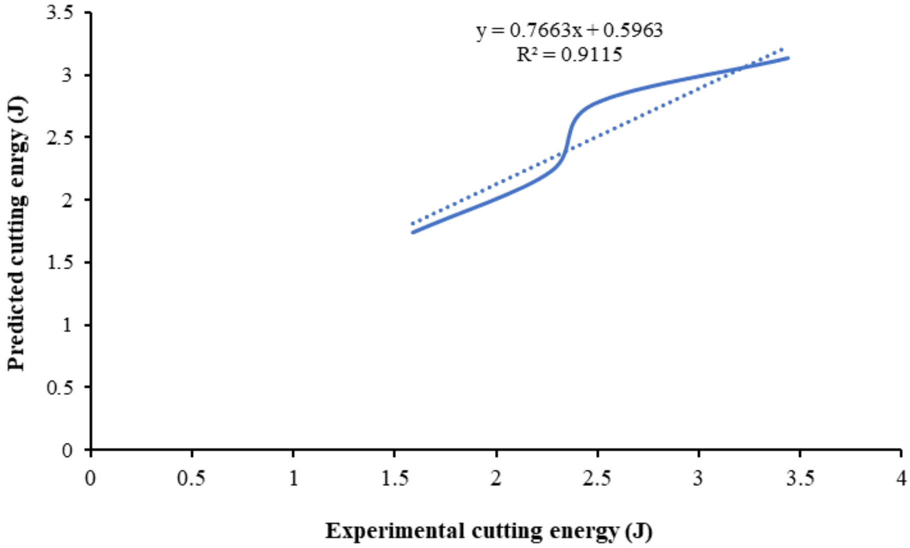

(b) Ifeken Di 400

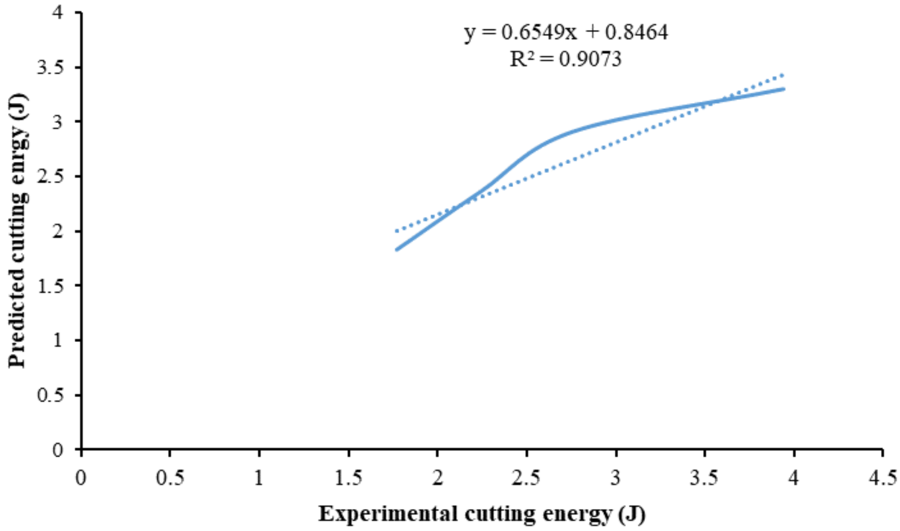

(c) Ifeken 400

Figure 8 Cutting energy model validation

5 Conclusion

The R^2 of all the model equations was closer to 1 than 0.7, indicating that the models can accurately predict the cutting torque, power, and energy consumed during kenaf and plant stalk harvesting.

The cutting torque, power, and energy consumed during kenaf harvesting increase steadily with increased maturity for all varieties of kenaf because the stem cross sectional area and the texture of the stalk constitute the crop cutting resistance, so more torque, power and energy are required during harvesting as the crop matures.

The highest cutting torque, power, and energy during the harvesting of Ifeken 400 ranged from 1.51 Nm to 3.36 Nm, 10.19 kW to 22.61 kW, and 1.77 Joules to 3.94 Joules. In contrast, harvesting Cuba 108 required less torque, power, and energy. The minimum energy, torque, power, and energy were consumed when harvesting Ifeken Di 400.

References

Ayadi, R., M. Hanana, R. Mzid, L. Hamrouni, M. L. Khouja, and A. S. Hanachi. 2017. Hibiscus cannabinus L.–kenaf: a review paper. *Journal of Natural Fibers,* 14(4): 466-484.

Ayorinde, A. T., G. Makanjuola, O. B. Aluko, O. K. Owolarafe, and L. A. Sanni. 2019. Performance evaluation of a kenaf decorticator. *CIGR Journal,* 21(1): 192-202.

Ayorinde, T. A., and Y. O. Olasebikan. 2020. Renewable Energy Source Adoption. *In:* Leal F. W., A. M. Azul, L. Brandli, S. A. Lange, & T. Wall. (eds.) *Affordable and Clean Energy.* Cham: Springer International Publishing.

Ayorinde, T. A., and O. K. Owolarafe. 2023a. Development of tractor mounted kenaf harvester. *Acta Technica Corviniensis-Bulletin of Engineering,* 16(2): 1-5.

Ayorinde, T. A., and O. K. Owolarafe. 2023b. Effect of operational parameters on the performance of a kenaf harvester. *Spanish Journal of Agricultural Research,* 21(4): e0209.

Chattopadhyay, P., and K. Pandey. 2001. PM—Power and machinery: impact cutting behaviour of sorghum stalk using a flail-cutter—a mathematical model and its experimental verification. *Journal of Agricultural Engineering Research,* 78(4): 369-376.

Dauda, S. M., D. Ahmad, A. Khalina, and O. Jamarie. 2015. Effect of cutting speed on cutting torque and cutting power of varying kenaf-stem diameters at different moisture contents. Pertanika Journal of Tropical Agricultural Science. 38 (4): 549 - 561

Dongdong, D. 2016. Research on mechanics properties of crop stalks: A review. *International Journal of Agricultural and Biological Engineering,* 9(6): 10-19.

Ghahraei, O., D., Ahmad, A. Khalina, H. Suryanto, and J. Othman. 2011. Cutting tests of kenaf stems. *Transactions of the ASABE,* 54(1): 51-56.

Guarnieri, A., C. Maglioni, and G. Molari. 2007. Dynamic analysis of reciprocating single-blade cutter bars. *Transactions of the ASABE,* 50(3): 755-764.

Gupta, C., and M. Oduori. 1992. Design of the revolving knife-type sugarcane base-cutter. Transactions of the American Society of Agricultural Engineers 35(6):1747-1751

Ishak, M., Z. Leman, S. Sapuan, A. Edeerozey, and I. Othman. 2010. Mechanical properties of kenaf bast and core fibre reinforced unsaturated polyester composites.In *IOP Conference Series: Materials Science and Engineering,* December 2009, Residence Hotel, UNITEN, Putrajaya, Malaysia.

Kushwaha, R., A. Vaishnav, and G. Zoerb. 1983. Shear strength of wheat straw. *Canadian Agricultural Engineering,* 25(2): 163-166.

McRandal, D., and P. McNulty. 1978. Impact cutting behaviour of forage crops I. Mathematical models and laboratory tests. *Journal of Agricultural Engineering Research,* 23(3): 313-328.

Müssig, J., S. Enke, H. Gusovius, C.Lühr, B. Uhrlaub, L. Dammer, and M. Carus. 2024. Mechanical separation of kenaf for composite applications–Evaluation of the total fibre line concept for field retted kenaf. *Industrial Crops and Products,* 208(2024):117870.

O'dogherty, M. 1982. A review of research on forage chopping. *Journal of Agricultural Engineering Research,* 27(4): 267-289.

Persson, S. 1987. *Mechanics of Cutting Plant Material*. American Society of Agricultural and Biological Engineers, ASABE, St. Joseph, Michigan.

Raji, A., and D. O. Aremu. 2017. Mechnaical properties of varieties of kenaf (Hibiscus Cannabius) stem. *Global Journal of Science Frontier Research*, 17(D6): 1-6

Sahni, R. K., and P. P. Jena. 2022. Effect of cutting velocity on cutting torque of varying black gram-stem diameters at different moisture content. The Pharma Innovation Journal, 11(9): 2625-2629.

Sheldon, A. 2014. *Preliminary evaluation of kenaf as a structural material.* Clemson University. PhD diss., Clemson University, Clemson City, SC, USA

Soleimani, N., M. R. Kamandar, F. Khoshnam, and A. Soleimani. 2023. Defining and modelling sesame stalk shear behaviour in harvesting by reciprocating cutting blade. *Biosystems Engineering,* 229: 44-56.

Srivastava, A. K., C. E. Goering, R. P. Rohrbach, and D. R. Buckmaster. 2006. Soil tillage. In *Engineering Principles of Agricultural Machines,* American Society of Agricultural Engineers Publication: Saint Joseph, MI**.**

Totten, D. S., and W. F. Millier. 1966. Energy and particle path analysis: forage blower and vertical pipe. *Transactions of the ASAE,* 9(5): 629-0636.

Uche, A. G., A. S. Nwabueze, M. J. Chibuike, and M. C. Joseph. 2018. Energy requirements for cutting of selected vegetables: A review. *CIGR Journal,* 20(4): 139-148.

Veikle, E. E. 2011. *Modeling the Power Requirements of A Rotary Feeding and Cutting System.* Ph.D. Thesis, University of Saskatchewan, Saskatoon, SK, Canada.

Yaghoobi, H., and A. Fereidoon. 2018. Modeling and optimization of tensile strength and modulus of polypropylene/kenaf fiber biocomposites using Box–Behnken response surface method. *Polymer Composites,* 39: E463-E479.

Yiljep, Y., and U. Mohammed. 2005. Effect of knife velocity on cutting energy and efficiency during impact cutting of sorghum stalk. Agricultural Engineering International: the CIGR EJournal, 7(7):1-10

Yilmaz, D., O. Kabas, I. Akinci, A. Ozmerzi, and M. I. Cagirgan. 2009a. Effect of moisture content and stalk section on some engineering parameters of closed capsule sesame stalks (Sesamum indicum L.). *Journal of Food, Agriculture and Environment,* 7 (3and4): 306-311.

Yilmaz, D., O. Kabas, I. Akinci, and M. I. Cagirgan. 2009b. Strength and deformation parameters of sesame stalk in relation to harvest. *Philippine Agricultural Scientist*, 92(1): 85-91.

Zastempowski, M., and A. Bochat. 2014. Modeling of cutting process by theshear-finger cutting block. *Applied Engineering in Agriculture,* 30(3): 347.

Zhao, X., C. Li, X. Chen, J. Cui, and B. Cao. 2022. Data-driven cutting parameters optimization method in multiple configurations machining process for energy consumption and production time saving. *International Journal of Precision Engineering and Manufacturing-Green Technology*, 9: 1-20.